

LONG RANGE PHASE COHERENCE IN THE CURRENT-CARRYING CHARGE DENSITY WAVE STATE

G. Grüner and A. Zettl

Department of Physics, University of California, Los Angeles, CA 90024, U.S.A.

Résumé - Diverses expériences comportant l'application conjointe de champs électriques continus (dc) et alternatifs (ac), $V = V_{dc} + V_{ac} \cos \omega t$ ont été effectuées sur le composé à chaîne linéaire $NbSe_3$: 1.) L'observation directe d'oscillations de courant avec la relation entre la fréquence f_0 et le courant d'onde de densité de charge donné par $I_{CDW}/f_0 = 2en(T)/n(0)$ où $n(T)$ est le nombre d'électrons condensés. 2.) Les sauts induits par le champ ac dans la courbe I-V. 3.) Les changements dans la réponse alternative quand $\omega/2\pi = f_0$. L'analyse de ces expériences conduit à assigner des réponses cohérentes à l'onde de densité de charge impliquant le volume total des échantillons et suggérant fortement une cohérence de phase à longue distance dans l'état porteur de courant. Alors que les descriptions à une seule coordonnée rendent compte de ces observations, elles n'expliquent pas le bruit large bande et la largeur finie des pics de bande étroite. Une comparaison avec de récentes tentatives théoriques d'explication de ces observations est donnée.

Abstract - Various experiments involving the joint application of ac and dc driving fields, $V = V_{dc} + V_{ac} \cos \omega t$ are reported in the linear chain compound $NbSe_3$: 1.) The direct observation of current oscillations with the relation between frequency f_0 and CDW current I_{CDW} given by $I_{CDW}/f_0 = 2en(T)/n(0)$ where $n(T)$ is the number of condensed electrons; 2.) the ac field induced steps in the I-V curve³; and 3.) changes in the ac response when $\omega/2\pi = f_0$. The analysis of these experiments leads to coherent CDW responses, which involve the total volume of the specimens, strongly suggesting long range phase coherence in the current carrying state. While the single coordinate descriptions account for these observations, they do not explain the broad band noise and the finite width of the narrow band peaks. A short comparison with recent theoretical attempts to explain these observations will be given.

1. INTRODUCTION

It is by now well established that the electric field E and frequency ω dependent conductivity observed in the linear chain compounds $NbSe_3$, TaS_3 , and NbS_3 is due to the collective response of the charge density wave (CDW) condensate.¹ In the current-carrying state, which develops when the applied dc electric field E exceeds a threshold field E_T , narrow band noise [i.e., sharp peaks in the Fourier transform of the time dependent current $I(t)$] is observed,² and the frequency of the fundamental ν is proportional to the current carried by the CDW.^{3,1}

Various models are proposed to account for these observations, all are related to the original suggestion by Fröhlich that the current is carried by the translational motion of the CDW as a whole.⁴ Both tunneling⁵ and classical⁶ motion have been proposed to describe the E and ω dependent response and both models also account for the narrow-band noise. In this paper we report various experiments which involve the joint application of ac and dc excitations in the current carrying CDW state. Our main conclusion, arrived at by analyzing our experimental results in terms of a classical (single particle) equation of motion,⁶ is that the whole specimen responds in a highly coherent manner, suggesting long-range phase coherence in the current-carrying CDW state.

2. FORMAL ANALOGY BETWEEN THE CLASSICAL MODEL OF CDW TRANSPORT AND THE JOSEPHSON JUNCTION

A phenomenological model⁶ treats the CDW as a classical object of mass m and charge e which moves in a periodic potential along the direction given by the CDW modulation. The period given by the CDW period λ . The equation of motion for the position is

$$\frac{dx^2}{dt^2} + \frac{1}{\tau} \frac{dx}{dt} + \frac{\omega_0^2}{Q} \sin Qx = \frac{eE}{m} \quad (1)$$

where $\tau^{-1} = \gamma/m$ with γ the damping constant $\omega_0^2 = k/m$, with k the restoring force and $Q = 2\pi/\lambda$. E is the applied electric field with $\theta = Qx$. Equation (1) can be reduced to a dimensionless form

$$\frac{d\theta}{dt^2} + \Gamma \frac{d\theta}{dt} + \sin\theta = \frac{E}{E_T} \quad (2)$$

With $\Gamma = (\omega_0^2)^{-1}$, $E_T = \lambda/2\pi \frac{m\omega_0^2}{e}$, and the time is measured in units of ω_0^{-1} . Equation (2) is formally identical to the equation which describes the behavior of resistivity coupled Josephson junctions⁷

$$\frac{d\phi^2}{dt^2} + G \frac{d\phi}{dt} + \sin\phi = \frac{I}{I_J} \quad (3)$$

where ϕ is the phase difference, I is the current across the junction, and $G = (RC\omega_J)^{-1}$, where R and C are the resistance and capacitance of the junction and $\omega_J = 2eI_J/\hbar C$. This formal analogy, also recognized by others,⁸ suggests a close formal correspondence between phenomena observed in Josephson junctions and in materials displaying CDW transport, when a combination of ac and dc driving fields is applied.

In this communication we report three observations related to the response of the CDW from a combination of applied ac and dc fields. All have the analogous effect in the Josephson junction literature⁹:

1. The direct observations^{10,11} of the current oscillations in the presence of an applied dc field. The phenomenon (observed earlier through narrow band noise studies) corresponds to the ac Josephson effect.
2. The effect of applied ac field on the dc I-V characteristics.¹² This phenomenon is usually called the Shapiro effect in the case of Josephson junctions; and
3. The effect of applied dc field on the ac response.¹³ A variety of such experiments (most of them involving microwave frequencies) are reported in the Josephson literature.

3. EXPERIMENTAL RESULTS AND ANALYSIS

The experiments were performed in the lower CDW state ($T < 59$ K) of the linear chain compound NbSe_3 . In all experiments the leads were applied to the ends of the NbSe_3 fibers, and therefore all observations refer to the response of the CDW along the chain direction. Conventional rf circuits were used to apply the driving fields and detect the dc response due to a combination of dc and ac applied fields $V = V_{dc} + V_1 \cos \omega t$. The real and imaginary parts of the frequency dependent conductivity, $\text{Re } \sigma(\omega)$ and $\text{Im } \sigma(\omega)$ were measured by an HP8754A Network Analyzer.

For the direct observation of the current oscillations, a current or a voltage pulse was applied to the sample, and the resulting response was displayed on an oscilloscope. Above the threshold field the response is characterized by a time dependent voltage $V(t) = V_0 + \Delta V g(t/t_0)$ where g is a periodic function of time t . A typical response is shown in the insert of Figure 1. Waveforms such as shown were used to evaluate the amplitude of the oscillating current ΔI and the total current I_{CDW} carried by the CDW. Figure 1 shows $\Delta I/I_{CDW}$ versus the applied electric field. The amplitude of the oscillating current just above threshold is a large fraction of the time average current. Figure 1 shows $\Delta I/I_{CDW}$ as a function of V/V_T obtained from both the current pulse and voltage pulse methods. At $V = 1.05 V_T$ the oscillating component has the same magnitude as the time-average CDW current. We were not able to evaluate ΔI and

I_{CDW} closer to V_T , but we expect $\Delta I/I_{CDW}$ to increase further as V approaches V_T from above. We conclude that in this specimen the active volume must be acting as a single domain with a single degree of freedom for the motion of the CDW. A similar conclusion has been reached by Fleming¹¹ recently.

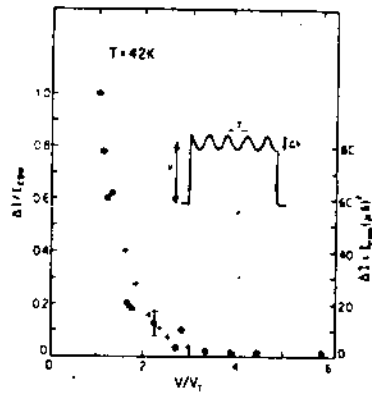


Fig. 1. The ratio between the amplitude of the oscillation ΔI and total CDW current I_{CDW} . \circ constant current pulses, $+$ constant voltage pulses. The insert shows a waveform somewhat above E_T .

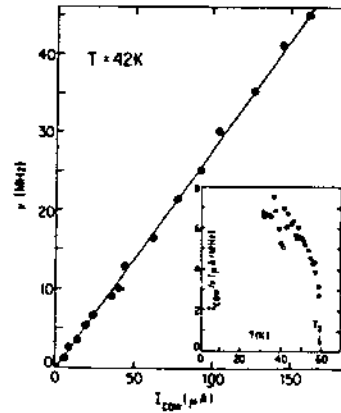


Figure 2. Noise frequency ν versus CDW current I_{CDW} . The insert shows I_{CDW}/ν measured at various temperatures.

The relation between I_{CDW} and the frequency of the current oscillation $\nu = E_0^{-1}$ is shown in Figure 2. As established by previous studies^{3,14} where the frequency of the current oscillations was measured at various applied fields, ν is proportional to the CDW current. Experimental data similar to those shown in the figure were taken at various temperatures, and the temperature dependence of I_{CDW}/ν is shown in the inset of Figure 2. The linear relation between I_{CDW} and ν has been interpreted by Monceau, Richard, and Renard³ as due to the motion of the CDW in a periodic potential. The CDW current is given by $I_{CDW} = n_c e V_d A$ where V_d is the drift velocity of the CDW, n_c is the density of electrons condensed in the CDW mode, and A is the cross section of the specimen. The oscillation frequency is $\nu = V_d/\lambda$, where λ is the wavelength of the CDW, leading to $I_{CDW}/\nu A = n_c e \lambda$. $n_c(T)$ varies as the temperature dependence of the gap, $\Delta(T)$ near to the Peierls transition temperature T_p . This temperature dependence gives strong support for transport by charge density waves. The relation between I_{CDW} and ν can also be written as I_{CDW}/ν per chain = $2e$ at $T = 0$. An alternative explanation,¹⁵ based on a moving soliton lattice, leads to I/ν per chain = $e/2$. While our experiments on $NbSe_3$ favor the first relation, complications associated with the presence of different types of chains and the partial removal of the Fermi surface by the transition suggest the relation should be checked in other compounds also.

In a second experiment, the dc I-V curve was recorded in the presence of an applied ac field $V_1 \cos \omega t$. Such rf-induced steps in the dc I-V characteristics of $NbSe_3$ were first reported by Monceau et al.,³ who found sharp peaks in the differential conductances in the nonlinear conductivity region, indicating interference effects between the applied ac frequency and the narrow-band noise frequency. Our experiments on $NbSe_3$ reported here, which were performed on samples with well-defined and uniform geometries, allow us to observe the steps directly on dc I-V plots. We observe interference effects approximately 100 times larger than those reported by Monceau et al.³

Figure 3 shows several dc I-V traces for $NbSe_3$ at $T = 42$ K, using a two probe mounting configuration. The excitation applied to the sample was of the form $V = V_{dc} + V_1 \cos \omega t$ with $\omega/2\pi = 100$ MHz. For $V_1 = 0$, a smooth, nonlinear I-V curve is observed. At higher values of V_1 , well-defined steps appear in the nonlinear region. The step height δV , as defined in the Figure, in general first increases with increasing V_1 , and then

decreases. The position of the $n = 1$ step (identified in the Figure) corresponds to a dc current $\langle I \rangle$ which, in the absence of external ac, yields an intrinsic oscillation of frequency $\nu = 100 \text{ MHz} = \omega/2\pi$. We also note the presence of harmonic steps corresponding to $n = 2$ (where $\nu = 200 \text{ MHz}$). The steps are thus clearly an interference effect between the intrinsic current oscillation and the externally applied rf excitation. The coherent current oscillations were observed directly during the same experimental run, and the fundamental oscillation frequency ν was found to vary as $\nu \sim I_{CDW}$, in agreement with previous studies.

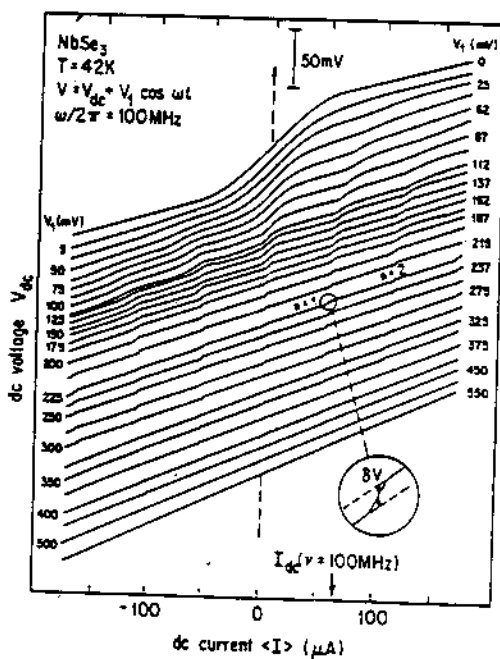


Fig. 3. dc I-V traces for NbSe_3 at 42 K in the presence of an applied rf field at frequency $\omega/2\pi = 100 \text{ MHz}$ and of amplitude V_1 . The step height δV is defined in the Figure. No Shapiro steps are seen for $V_1 = 0$, while the maximum step height is at approximately $V_1 = 100 \text{ mV}$. The arrow indicates the dc current which yields a noise frequency $\nu = 100 \text{ MHz}$. n is the step index (see text).

In Figure 4 we show the detailed form of the $n = 1$ step height δV as a function of V_1 , for a different sample and with $\omega = 210 \text{ MHz}$. We find δV resembles a decaying oscillatory function, with well-defined maxima and minima.

Such oscillatory behavior of δV is characteristic of the response observed in Josephson junctions.¹⁶ The solution of Eq. (2) in the high frequency limit leads, in direct analogy to Eq. (3), to

$$\delta V = \alpha V_T(\omega=0) 2 |J_1[V_1 \omega_0^2 \tau / \omega V_T(\omega=0)]| \quad (5)$$

for the $n = 1$ step height. The parameter α represents the volume fraction of the sample which responds collectively to the external field. Approximate solutions in the low frequency limit also lead to an oscillatory behavior. In Figure 4 (which is for $\omega/2\pi = 210 \text{ MHz}$), we have plotted Eq. (5) with chosen parameters $\omega_0^2 \tau = 503 \text{ MHz}$ and $\alpha = 0.17$. V_T is fixed by experimental conditions at 24 mV. The positions of the maxima and minima of the Bessel function of Eq. (5) are in remarkably good agreement with the experimental data. The value of the cross-over frequency $\omega_0^2 \tau / 2\pi$ deduced from this fit is 80 MHz, in reasonable agreement with the value of 45 MHz obtained from frequency-dependent conductivity studies.¹⁷ The value of $\alpha = 0.17$ indicates that a large fraction of the sample is responding coherently to the external perturbation. Analysis of similar data for another sample yielded an even higher value of $\alpha = 0.60$, which

corresponds to 60% of the sample volume being phase coherent. The high coherence is in agreement with the previous experiment of the current oscillations^{10,11} and switching phenomena¹⁸ of NbSe₃.

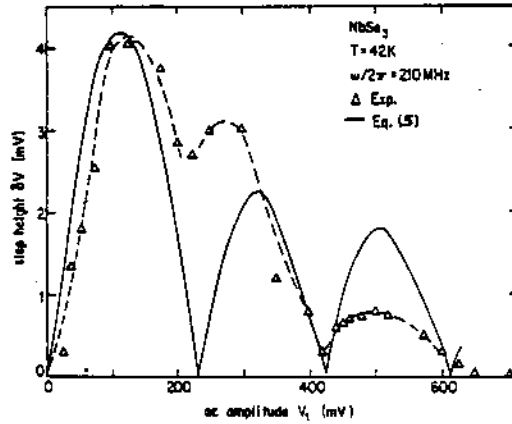


Fig. 4. Step height δV versus amplitude V_1 of the applied rf signal. The rf frequency is 210 MHz and the step index $n = 1$ (see text). The solid line is Eq. (5), with parameters given in the text. The dashed line is a guide for the eye.

The step heights, as shown in Figure 4, are strongly frequency dependent. We have made measurements similar to those shown in Figure 3 at different values of ω , and we find that the general form of δV versus V_1 , including the positions of the peak maxima and minima, remains essentially unchanged between $\omega/2\pi = 10$ MHz and 200 MHz. The maximum step height attained, however, strongly decreases with decreasing ω . In Figure 5 we show the maximum step height δV_{\max} .

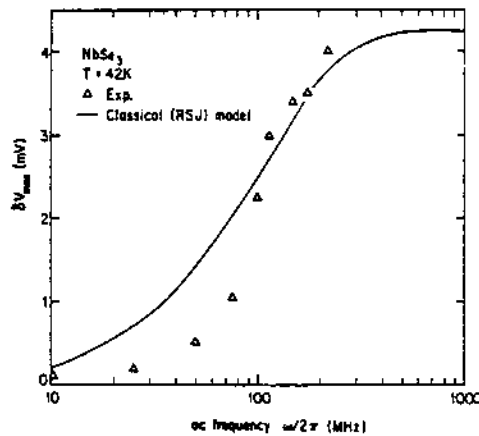


Fig. 5. Maximum step height δV_{\max} attained, versus rf frequency. The solid line is the prediction of the RSJ model of Josephson tunnel junctions.

The strong frequency dependence of δV_{\max} as shown in Figure 5 indicates that a low frequency solution is most appropriate below 200 MHz. Neglecting the first term in Eq. (2) yields the standard RSJ (resistively shunted-junction) model of Josephson junction. In the CDW case this corresponds to neglecting the effects of inertia (overdamped response). The solid line in Figure 5 is the frequency dependence of δV_{\max} , as calculated^{7,9,15} for the RSJ model in the overdamped limit. The value of $\omega_0^2\tau/2\pi = 45$ MHz obtained from the fit is in good agreement with that deduced from the frequency

dependence of the low-field ac conductivity,¹⁷ and consistent with that deduced from the analysis of Figure 4.

In the third type of experiment the ac response, i.e., the real and imaginary parts of the complex conductivity $\text{Re } \sigma(\omega)$ and $\text{Im } \sigma(\omega)$, was measured. The dielectric constant is defined as $\epsilon(\omega) = \text{Im } \sigma(\omega) / \omega$. Again, in the presence of an applied field $E > E_T$, interference peaks are expected to occur where $\omega/2\pi = v = t_0^{-1}$. Figures 6a and 6b show ϵ and $\text{Re } \sigma(\omega)$, both measured at a frequency $\omega/2\pi = 3.2$ MHz. Large inductive dips occur in ϵ at frequencies v , $2v$, and $v/2$. $\text{Re } \sigma(\omega)$ shows strong jump-like increases at these frequencies. Only a semiquantitative analysis can be given for these types of interference effects, but again the conclusion is that the whole sample volume is involved in a highly coherent response.

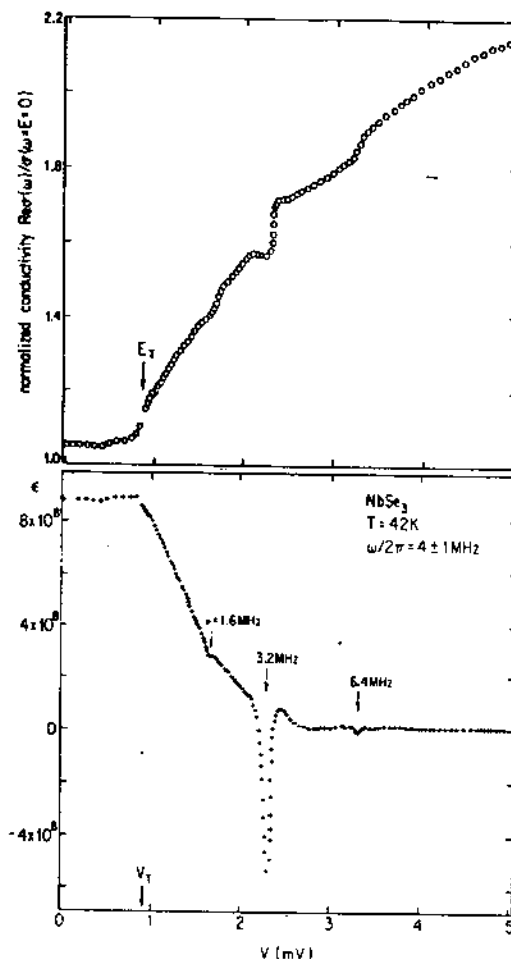


Fig. 6. Ac conductivity at $\omega/2\pi = 3.2$ MHz in the presence of applied dc field. a) Real part $\text{Re } \sigma(\omega)$, b) dielectric constant $\epsilon(\omega) \sim \text{Im } \sigma(\omega) / \omega$.

4. CONCLUSIONS

Experiments reported in this paper strongly suggest that in the sliding charge density wave mode the whole specimen responds to ac and dc driving fields in a highly coherent manner, indicative of a long range phase coherence in the current carrying CDW state. Analysis of experiment in terms of single nonlinear equation describes surprisingly well the various aspects of response which are associated with the internal oscillations of the velocity of CDW. We believe that any theory which accounts for nonlinear and

frequency dependent phenomena, and which describes the current oscillations, should also account for interference effects. The semiconductor model proposed by Bardeen⁵ is therefore also compatible with our experimental findings.

Both descriptions also consider the CDW response in terms of the time dependence of the average phase, with time dependent internal deformations is thought to be responsible for pinning (with appropriate dependence of the threshold field on the impurity concentration) in the thermodynamic limit. The dynamics of the internal deformations is most probably responsible for the broad band noise observed in the current carrying state.

The question whether a rigid CDW would have no pinning and damping (and thus have an infinite conductivity for $E \rightarrow \infty$) has not been resolved yet, but it appears likely that both long range coherence and local deformations of the phase are of importance in the understanding of charge density wave transport phenomena.

We also note that the experiments reported here demonstrate that the whole specimen responds as one unit with a single degree of freedom in the current-carrying state. Questions associated with the effects of finite sample size on the measured parameters are therefore expected to be important. The condensate is characterized by coherence and correlation lengths of the order of microns or more, and when the length of the sample is comparable to these characteristic distances, strong boundary effects are expected to occur. Our preliminary measurements of the threshold field E_T as a function of sample length indeed indicate that such effects are important, with lengths scales of the order of 10^{-2} cm.

We wish to thank John Bardeen, W. G. Clark, T. Holstein, R. Klemm, J. R. Schrieffer, and A. Zawadowski for useful discussions. This research was supported by the NSF Grant DMR 81-03085.

REFERENCES

1. See, for example, R. M. Fleming, in Physics in One Dimension, Springer Series in Solid State Sciences, Vol. 23, eds., J. Bernasconi and T. Schneider (Springer Verlag, New York, 1981); N. P. Ong, Con. J. Phys. **60**, 757 (1982); G. Gruner, Mol. Cryst. Liq. Cryst. **87**, 17 (1982).
2. R. M. Fleming and C. C. Grimes, Phys. Rev. Lett. **42**, 1423 (1979).
3. P. Monceau, J. Richard, and M. Renard, Phys. Rev. Lett. **45**, 43 (1980).
4. H. Fröhlich, Proc. Roy. Soc. **A223**, 296 (1954).
5. John Bardeen, Phys. Rev. Lett. **42**, 1498 (1979), **45**, 1978 (1980); Molecular Crystals and Liquid Crystals **81**, 719 (1981).
6. G. Gruner, Z. Zawadowsky, and P. M. Chaikin, Phys. Rev. Lett. **46**, 511 (1981). Some of the details of the model have been worked by P. Monceau et al., Phys. Rev. B **25**, 931 (1982).
7. D. E. McCumber, J. Appl. Phys. **39**, 3113 (1968); W. C. Stewart, Appl. Phys. Lett. **12**, 277 (1968).
8. S. N. Artemenko and A. F. Volkov, Zh. Exp. Teor. Fiz. **81**, 1872 (1981) [Sov. Phys. -JETP **54**, 992 (1981)]; E. Ben Jacob (to be published).
9. See, for example, P. E. Lindelof, Rep. Prog. Phys. **44**, 60 (1981).
10. John Bardeen, E. Ben Jacob, A. Zettl, and G. Gruner, Phys. Rev. Lett. **49**, 493 (1982).
11. R. M. Fleming, Sol. State Commun. **43**, 167 (1981).
12. A. Zettl and G. Gruner (submitted to Phys. Rev. Lett.).
13. A. Zettl and G. Gruner (to be published).
14. M. Weger, G. Gruner, and W. G. Clark, Sol. State Commun. **35**, 243 (1980).
15. Per Bak, Phys. Rev. Lett. **48**, 672 (1982). A model based on impurity induced tunneling between states with k_F and $-k_F$ leads to I_{CDW}/v per chain = e at $T = 0$.
16. S. Shapiro, Phys. Rev. Lett. **11**, 80 (1963).
17. G. Gruner, A. Zettl, W. G. Clark, and John Bardeen, Phys. Rev. B **24**, 7247 (1981).
18. A. Zettl and G. Gruner, Phys. Rev. B **26**, 2298 (1982).